IHRT IFAC TU

International Federation of Automatic Control – IFAC

Institute for Handling Devices and Robotics - IHRT
Vienna University of Technology

6th IFAC Symposium on Robot Control

SYROCO '00

September 21st - 23rd, 2000
Vienna, Austria

Preprints

VOLUME II

Edited by:

Peter Kopacek
Institute for Handling Devices and Robotics
Vienna University of Technology

CHAOTIC BEHAVIOR IN THE PSEUDOINVERSE CONTROL OF REDUNDANT AND HYPER-REDUNDANT ROBOTS

Fernando B. M. Duarte*
J. A. Tenreiro Machado**

**Dept. of Mathematics, Scholl of Technology, Polytechnic Institute of Viseu, 3500 Viseu, Portugal - e-mail: fduarte@mat.estv.ipv.pt*
***Dept. of Electrical Engineering, Institute of Engineering, Polytechnic Institute of Porto 4200-072 Porto, Portugal - e-mail: jtm@dee.isep.ipp.pt*

Abstract: Several kinematic control algorithms for redundant manipulators adopt generalized inverse matrices. In this line of thought, the generalized inverse control scheme is tested through experiments that reveal the difficulties that often arise. The experiments confirm the non-linear and chaotic performance of the algorithm and give a deeper insight towards the future development of superior trajectory control systems.

Keywords: Chaotic behavior, Chaos, Fractal, Redundant Manipulators, Robots.

1. INTRODUCTION

A kinematically redundant manipulator is a robotic arm possessing more degrees of freedom (*dof*) than those required to establish an arbitrary position and orientation of the end effector (Conkur and Buckingham, 1997; Chiaverini, 1997; Yoshikawa, 1988). When a manipulator is redundant, it is anticipated that the inverse kinematics admits an infinite number of solutions. This implies that, for a given location of the manipulator's end effector, it is possible to induce a self-motion of the structure without changing the location of the gripper. Thus, the arm can be reconFig.d to find better postures for an assigned set of task requirements.

Many techniques for solving the kinematics of redundant manipulators that have been suggested control the end effector indirectly, through the rates at which the joints are driven, using the pseudoinverse of the Jacobian (Klein and Huang, 1983; Duarte, Machado, 1999). Nevertheless, these algorithms lead to a kind of chaotic motion with unpredictable arm configurations. Therefore, an important area of research remains open.
Having these ideas in mind, the paper is organized as follows. Section 2 develops the formalism for the kinematics and dynamics of redundant manipulators. Based on these concepts, section 3 presents several experiments with the kinematics and dynamics of redundant robots. Section 4 analyses the chaotic phenomena revealed by the trajectory planning algorithms. Finally, section 5 draws the conclusions.

2. KINEMATIC AND DYNAMIC MODELLING

2.1 Problem Formulation

We consider a manipulator with n *dof* whose joint variables are denoted by $\mathbf{q} = [q_1,..., q_n]^T$. We assume that a class of tasks we are interested in can be described by m variables $\mathbf{x} = [x_1, ..., x_m]^T$ ($m < n$) and the relation between $\mathbf{q}$ and $\mathbf{x}$ is:

$$\mathbf{x} = f(\mathbf{q}) \tag{1}$$

where f is a function representing the direct kinematics. Differentiating (1) with respect to time yields:

$$\dot{\mathbf{x}} = \mathbf{J}(\mathbf{q})\dot{\mathbf{q}} \tag{2}$$

where $\mathbf{J}(\mathbf{q}) = \partial f(\mathbf{q})/\partial \mathbf{q} \in \Re^{m \times n}$.

Several approaches for solving redundancy that have been proposed (Nakamura, 1991; Chung W. J., *et al.*, 1994) are based on the inversion of equation (2). A solution in terms of the joint velocities, is sought as:

$$\dot{\mathbf{q}} = \mathbf{J}^{\#}(\mathbf{q})\dot{\mathbf{x}} \tag{3}$$

where $\mathbf{J}^{\#}$ is one of the generalized inverses (Doty, *et al.*, 1993) of $\mathbf{J}$. In the closed-loop pseudoinverse's method (CLP) the joint positions are computed through the time integration of the velocities according with the block diagram depicted in Fig. 1.

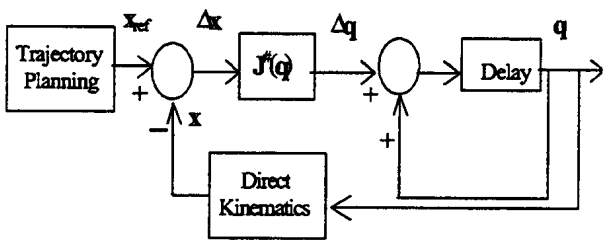

Fig. 1. Block diagram of the closed-loop inverse kinematics.

An aspect revealed by the CLP is that repetitive trajectories in the operational space do not lead to periodic trajectories in the joint space (Siciliano, 1990; Seereeram and Wen 1995). This is an obstacle for the solution of many tasks because the resultant robot configurations have similarities with those of an chaotic system. To solve this lack of repetition several others methods were proposed (Seereeram and Wen 1995; Roberts and Maciejewski 1993). Nevertheless, clear conclusions about the nature of the phenomena involved when using $\mathbf{J}^{\#}$ are still lacking.

2.2 Kinematics and Dynamics

The Jacobian of a k-link planar manipulator has a simple recursive nature according with the expressions:

$$\mathbf{J} = \begin{bmatrix} -l_1 S_1 & \cdots & -l_1 S_1 - l_2 S_{12} - \cdots - l_k S_{1k} \\ l_1 C_1 & \cdots & l_1 C_1 + l_2 C_{12} + \cdots + l_k C_{1k} \end{bmatrix} \qquad (4)$$

where l_i is the length of link i, $S_{ik} = Sin(q_i + \cdots + q_k)$ and $C_{ik} = Cos(q_i + \cdots + q_k)$.

The symbolic formulae for the inverse dynamics of a k-link planar robot can be formulated recursively as:

$$\begin{aligned} T = & \sum_{i=1}^{n} (m_i (\sum_{p=1}^{i-1} (If\,[j > p, B1 = 0, B1 = 1]; {l_p}^2 \sum_{u=1}^{p} \ddot{q}_u B1) \\ & + {r_i}^2 \sum_{u=1}^{i} \ddot{q}_u + \sum_{p=2}^{i} (\sum_{k=1}^{p-1} (If\,[p > i-1, B2 = 0, B2 = 1]; \\ & [If\,[p == i, B3 = 1, B3 = 0]; If\,[j > k, B4 = 0, B4 = 1]; \\ & If\,[(j >= k+1 \&\& j <= p), B5 = 1, B5 = 0]; \\ & l_k (l_p B2 + r_p B3)((-S_{k+1..p} ((\sum_{u=k+1}^{p} \dot{q}_u)^2 + \\ & 2 \sum_{u=1}^{k} \dot{q}_u \sum_{u=k+1}^{p} \dot{q}_u) + C_{k+1..p} (\sum_{u=1}^{p} \ddot{q}_u + \sum_{u=1}^{k} q_u)))B4 + \\ & (S_{k+1..p} (\sum_{u=1}^{k} \dot{q}_u)^2 + C_{k+1..p} \sum_{u=1}^{k} \ddot{q}_u)B5 + \\ & g(\sum_{p=1}^{i-1} (If\,[j > p, B1 = 0, B1 = 1]; l_p C_{1..p} B1) + r_i C_{1..i}))) \end{aligned} \qquad (5)$$

where T are the joints torques $B1$ to $B5$ are logical conditions, m_i is the mass of link i, r_i is the distance from the joint axis to the link center of mass and g is the acceleration due to gravity.

During the experiments, it is considered $r=(x_1+x_2)^{1/2}$ $\Delta t = 0.001$ sec, $l_1 + l_2 + l_3 + \ldots + l_k = l_T$, $l_1 = l_2 = l_3 = \ldots = l_k$, $m_1 + m_2 + \ldots + m_k = m_T$, $m_1 = \ldots = m_k$, $l_T = 3$ and $m_T = 3$.

3. TRAJECTORY CONTROL

In this section we analyze the performances of the CLP method. In this line of thought, we study the joint trajectories for the redundant $3R$ robot, when subjected to a repetitive circular trajectory in the operational space with radius ρ (Fig. 2). We conclude that the manipulability $\mu=(\det(JJ^T))^{1/2}$ (Yoshikawa, 1988; Nakamura, 1991) is non-optimal and the joint trajectories exhibit sudden changes, which impose large joint velocities. Moreover, the joint trajectories are non-repetitive leading to a kind of chaotic performance.

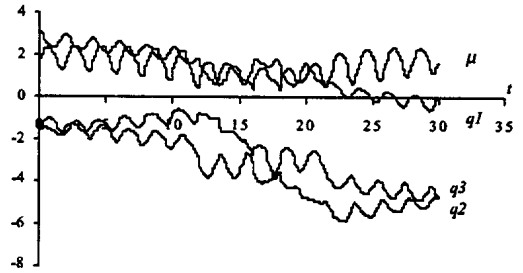

Fig. 2. The $3R$-robot joint positions *versus* time using the CLP method for $r=1$, $\rho=0.5$.

In a second experiment we analyze the robot inverse dynamics when subjected to the repetitive circular trajectory in the operational space. Fig. 3 shows the resulting the joint torques for the $3R$ manipulator when the CLP method is used. It is clear that the dynamics follows the kinematic non-repetitive responses and exhibits the same type of problems. For other robots, such as the $4R$ and $5R$ hyper-redundant manipulators, we get similar conclusions.

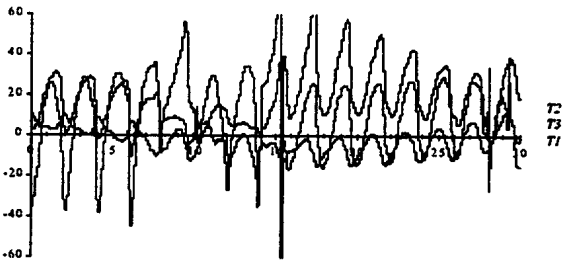

Fig. 3. The $3R$-robot joint torques *versus* time using the CLP method for $r=1$, $\rho=0.5$. Max (T_1) =158.1 *Nm* at *t=15.3 sec.* Max (T_2) =67.6 *Nm* at *t=15.3 sec.* Max (T_3)=14.7 *Nm* at *t=11.5 sec.*

4. CHAOTIC RESPONSES OF THE PSEUDOINVERSE ALGORITHM

It was shown previously that the CLP algorithm leads to unpredictable arm configurations, with responses similar to those of a chaotic system (Duarte and Machado, 1999).

For example, Fig. 4 depicts the phase-plane joint trajectories for the $3R$-robot when repeating a circular motion, with center at $r = 1$, radius $\rho = 0.1$ and frequency $\omega_0 = 3$ under the CLP scheme. Besides the motion drift, leading to different trajectory loops, we have points that are 'avoided'. Such points correspond to arm configurations where several links are aligned. This characteristic is inherent to the pseudoinverse matrix. Therefore, in order to gain further insight into the chaotic nature of the phenomena, the robots under investigation were required to follow the cartesian repetitive circular motion for several radial distances r. The phase-plane joint trajectories were analyzed and their fractal dimension (*dim*) estimated using the box-counting method:

$$\dim S = \lim_{\varepsilon \to 0} \frac{\ln N(\varepsilon)}{\ln (1/\varepsilon)} \qquad (6)$$

where $N(\varepsilon)$ denotes the smallest number of bi-dimensional boxes of side length ε required in order to completely cover the plot surface S (Theiler, 1990). The results (Fig. 5) show that:

- for the pseudoinverse method we have $dim \approx 2$ due to the position and velocity drifts, in contrast with the 'standard' case where we have $dim \approx 1$.
- the fractal dimension diminishes near the maximum radial distance (*i.e.* $r = 3$).
- for each type of robot the fractal dimension is nearly the same, for all joints.
- At the singular points, for each type of robot, *dim* has a variation.

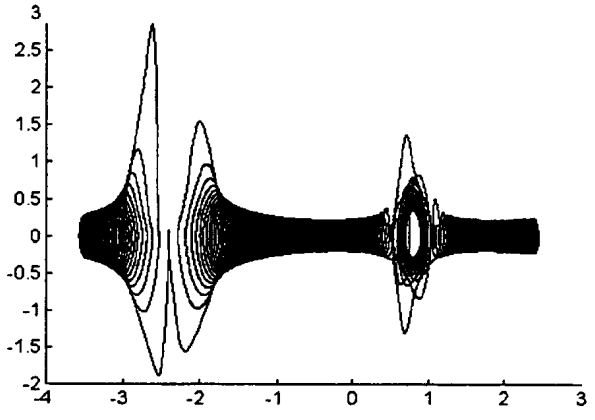

Fig. 4. Phase plane $\{q_1, \dot{q}_1\}$ trajectory for the $3R$- robot joint one under CLP method at $r = 1$, $\rho = 0.1$, $dim = 1.62$.

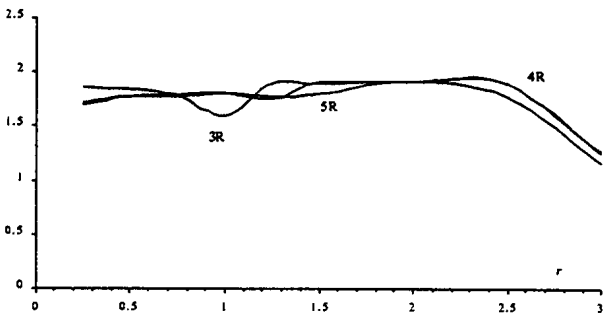

Fig. 5. Fractal dimension *dim* of the kinematic phase-plane *versus* the radial distance *r* with de CLP method, $\rho = 0.1$.

The chaotic motion is due to the contribution of the Jacobian pseudoinverse to the manipulator inner motion. Nevertheless, a deeper insight into the nature of this motion must be envisaged. Therefore, four experiments were devised to establish the texture of the Jacobian null space.

In a first experiment, the robot is required to start in an initial random configuration with $q_i \in]-\pi,\pi]$ $(i = 1, 2, 3)$ and to attain a fixed point in the operation space under the control of the CLP scheme. After elapsing the trajectory transient, the final robot joint positions are recorded. The experiment is repeated in order to establish a statistical characterization of the manipulator steady-state configuration. For a given desired position in the operational space, we conclude that the possible robot configurations have distinct probabilities (Fig. 6).

The second set of experiments is similar to the previous one with the exception that, in this case, the robot hand is following a circular repetitive motion with radius $\rho = 0.5$ and center at r. The set of joint positions recorded after elapsing the initial transient lead to the histogram shown in Fig.7.

From the two experiments we conclude that:

- The possible robot configurations have distinct probabilities.
- The probability distribution varies with ρ.
- The histograms for the second and third axis are similar while the first axis has other characteristics.
- The singular point $r = 1$ leads to a different chart region and a larger dispersion of the probability distribution. Moreover, this point represents the boundary of two distinct regions namely $0 < r < 1$ and $1 < r < l_T - \rho$.

In a third set of experiments the frequency response of the CLP method for the robot was computed numerically. Fig. 8 depict the resulting amplitude Bode diagrams for $r = 2$ and $\rho \in \{0.10, 0.25, 0.50, 0.75, 1.00\}$. It is clear that the transfer matrix for the *MIMO* system $(x_{ref}, y_{ref}) \rightarrow (q_1, q_2, q_3)$ depends strongly on the amplitude of the 'exciting' signal ρ. Moreover, the Bode diagrams reveal that the CLP method presents distinct gains for the joint variables, according with the frequency. This conclusion is consistent

with the phase-plane charts, that revealed low frequency drifts, while responding to an higher frequency signal input. Repeating the experiments for the $4R$ hyper-redundant robot leads to the same conclusions. For example, Fig. 9 show the statistical distribution of the joint variables for the $4R$ robot under the CLP with ρ=0.

In a fourth group of experiments the Fourier transform of the robot joint velocities, after elapsing a initial transient, is. calculated for a large number of cycles of circular repetitive motion with frequency $\omega_0 = 3$. Fig. 10 shows the results for the $3R$ robot versus the radial distance r the center of the circle with radius ρ=0.25. Once more we verify that for $0 < r < 1$ we get a signal energy distribution along all frequencies, while for $r > 1$ the major part of the signal energy is concentrated at the fundamental and multiple harmonics. Moreover, the DC component, responsible for the position drift, reduces considerably.

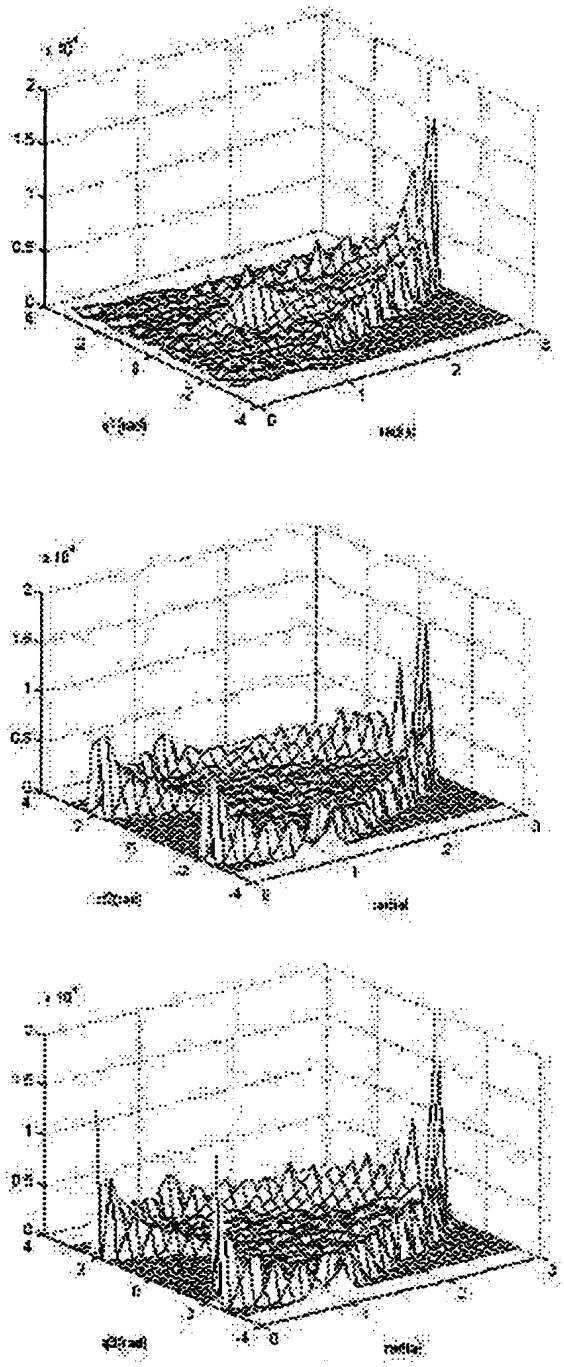

Fig. 6. Statistical distribution of the robot $3R$ joint positions *vs* the radial distance r for ρ=0.

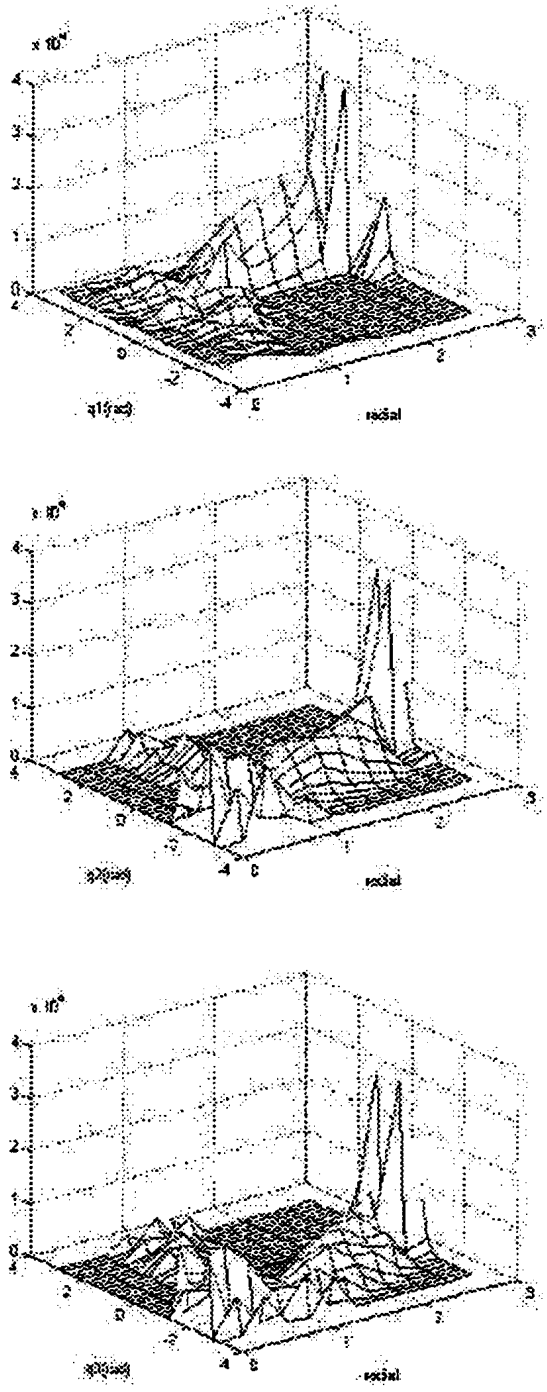

Fig. 7. Statistical distribution of the robot $3R$ joint positions *vs* the radial distance r for ρ=0.5.

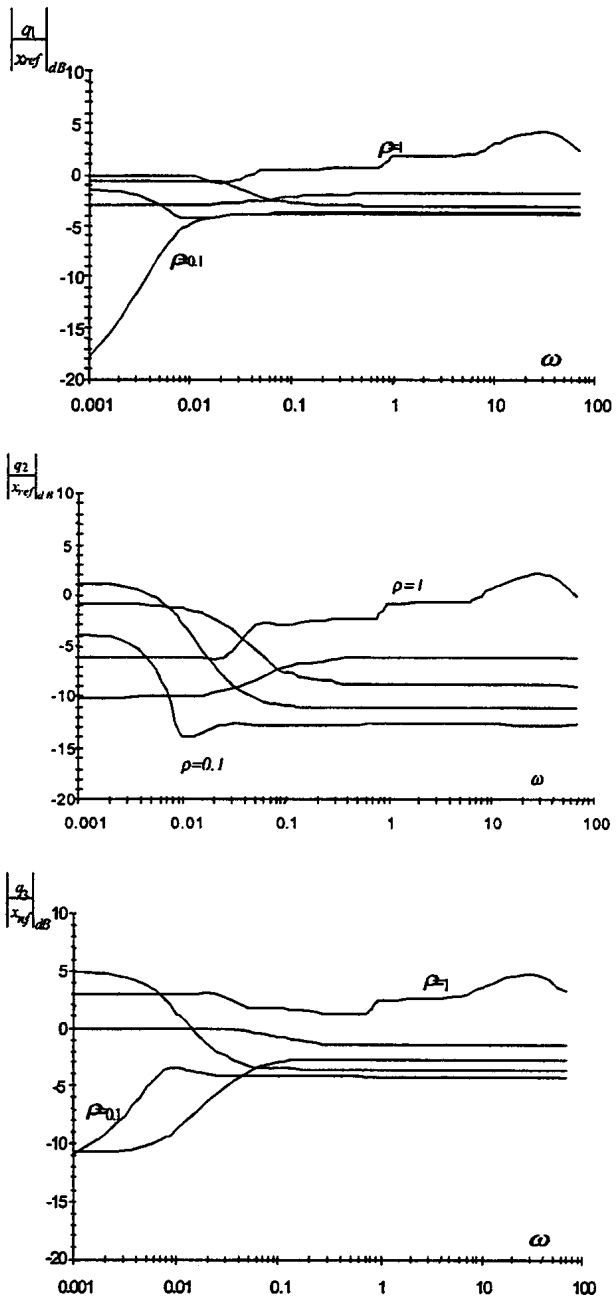

Fig. 8. Frequency response of the CLP method for the $3R$ robot, $r=2, \rho \in \{0.10, 0.25, 0.50, 0.75, 1.00\}$.

5. CONCLUSIONS

This paper discussed several aspects of the phenomena generated by the pseudoinverse-based trajectory control of redundant manipulators. Furthermore, the study addressed both the kinematics and dynamics in order to test the influence of each model.

The CLP scheme leads to non-optimal responses, both for the manipulability and the repeatability. Bearing these facts in mind, the fractal dimension of the responses was analyzed showing that it is independent of the robot joint. In fact, the chaotic motion depends on the operational space point and on the amplitude of the exciting repetitive motion. In this perspective, the chaotic responses where analyzed from different point of views namely, phase-plane, statistics and frequency response. The results are consistent and represent a step towards the development of superior trajectory planning algorithms for redundant and hyper-redundant manipulators.

REFERENCES

Chiaverini, S. (1997). Singularity-Robust task-Priority Redundancy Resolution for Real Time Kinematic Control of Robot Manipulators. *IEEE Transactions Robotics Automation*, **vol. 13**, pp. 398-410.

Chung W. J., and Y. Youm and W. K. Chung (1994). Inverse Kinematics of Planar Redundant Manipulators via Virtual Links With Configuration Index. *Journal of Robotic Systems*, vol. 11, pp. 117-128.

Conkur, E. S. and R. Buckingham (1997). Clarifying the Definition of Redundancy as Used in Robotics. *Robotica*, **vol. 15**, pp. 583-586.

Doty, K. L. and C. Melchiorri and C. Bonivento (1993). A Theory of Generalized Inverses Applied to Robotics. *Int., Journal of Robotics Research*, **vol. 12**, pp. 1-19.

Duarte, F. B. and J. A T. Machado (1999). Chaotic Phenomena and Performance Optimization in the Trajectory Control of Redundant Manipulators. In *Recent Advances in Mechatronics*, Springer-Verlag, Eds O. Kaynak et al..

Duarte, F. B. and J. A. T. Machado (2000). Chaos Dynamics in the trajectory Control of Redundant Manipulators. *IEEE International Conference on Robotics and Automation*, S. Francisco, USA.

Klein, C. A. and C. C. Huang (1983). Review of Pseudoinverse Control for Use With Kinematically Redundant Manipulators. *IEEE Trans. Syst. Man, Cyber.*, **vol. 13**, pp. 245-250.

Machado, J. A. T. and F. B. Duarte (1998). Redundancy Optimization for Mechanical Manipulators. *5th IEEE International Workshop on Advanced Motion Control, Coimbra, Portugal.*

Nakamura, Y. (1991). *Advanced Robotics: Redundancy and Optimization*, Addinson-Wesley.

Roberts, R. G. and A. A. Maciejewski (1993). Repeatble Generalized Inverse Control Strategies for Kinematically Redundant Manipulators. *IEEE Transactions on Automatic Control*, **vol. 38**, n° 5, pp. 689-699.

Seereeram, S. and J. T. Wen (1995). A Global Approach to Path Planning for Redundant Manipulators. *IEEE Tran Robotics Automat.*, **vol. 11**, pp.152-159.

Siciliano B (1990). Kinematic Control of Redundant Robot Manipulators: A Tutorial. *Journal of Intelligent and Robotic Systems*, **vol. 3**, pp. 201-212.

Theiler, J. (1990). Estimating Fractal Dimension. *Journal Optical Society of America*, vol. 7, n°6, pp. 1055-1073.

Yoshikawa, T. (1988). *Foundations of Robotics: Analysis and Control*, MIT Press.

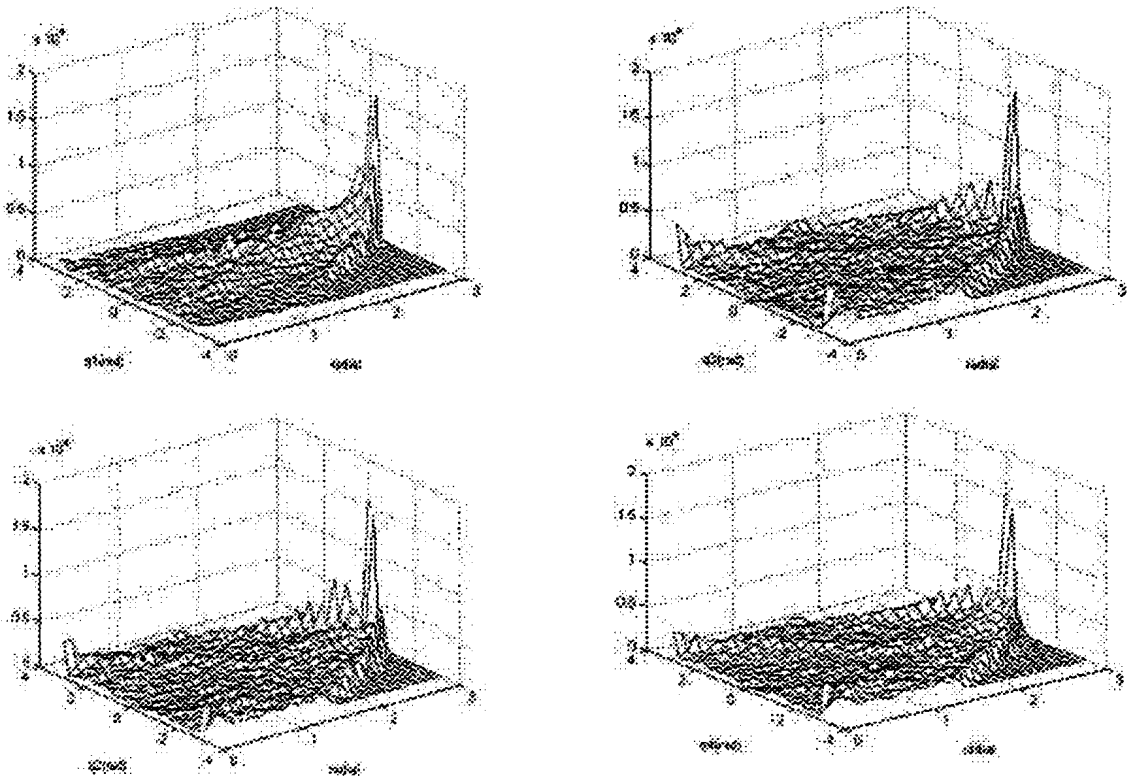

Fig. 9. Statistical distribution of the robot $4R$ joint positions *vs* the radial distance r for ρ=0.

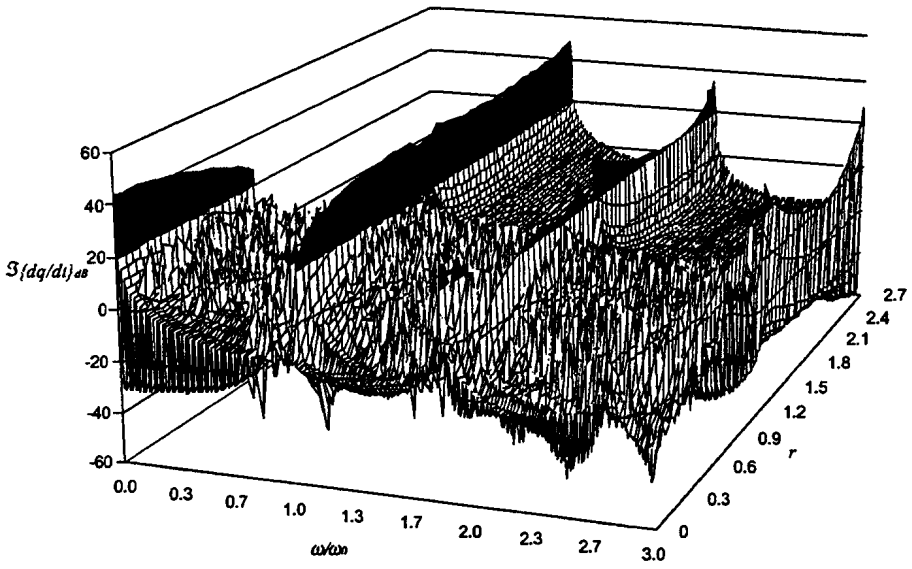

Fig. 10. Fourier transform of the robot $3R$ joint one velocity, for 500 cycles, *vs* the radial distance r and frequency ratio ω/ω_0, for ρ=0.25